MicroRNA-mediated disruption of dendritogenesis during a critical period of development influences cognitive capacity later in life

Quan Lin[a,b,1], Ravikumar Ponnusamy[c], Jocelyn Widagdo[d,e], Jung A. Choi[b], Weihong Ge[b], Christine Probst[b], Tyler Buckley[b], Mimi Lou[f], Timothy W. Bredy[d], Michael S. Fanselow[b,g,h], Keqiang Ye[i], and Yi E. Sun[a,b,1]

[a]Stem Cell Translational Research Center, Tongji Hospital, Tongji University School of Medicine, Shanghai, China 200092; [b]Department of Psychiatry and Behavioral Sciences, Intellectual Development and Disabilities Research Center, University of California, Los Angeles, CA 90095; [c]Veterans Affairs Palo Alto Division, Department of Psychiatry, Stanford University School of Medicine, Palo Alto, CA 94304; [d]Queensland Brain Institute, The University of Queensland, Brisbane, QLD 4072, Australia; [e]Clem Jones Centre for Ageing Dementia Research, The University of Queensland, Brisbane, QLD 4072, Australia; [f]School of Pharmacy, University of Southern California, Los Angeles, CA 90033; [g]The Brain Research Institute, University of California, Los Angeles, CA 90095; [h]Department of Psychology, University of California, Los Angeles, CA 90095; and [i]Department of Pathology and Laboratory Medicine, Center for Neurodegenerative Diseases, Emory University School of Medicine, Atlanta, GA 30322

Edited by Thomas C. Südhof, Stanford University School of Medicine, Stanford, CA, and approved July 6, 2017 (received for review April 25, 2017)

The prenatal period of cortical development is important for the establishment of neural circuitry and functional connectivity of the brain; however, the molecular mechanisms underlying this process remain unclear. Here we report that disruption of the actin–cytoskeletal network in the developing mouse prefrontal cortex alters dendritic morphogenesis and synapse formation, leading to enhanced formation of fear-related memory in adulthood. These effects are mediated by a brain-enriched microRNA, miR-9, through its negative regulation of diaphanous homologous protein 1 (Diap1), a key organizer of the actin cytoskeletal assembly. Our findings not only revealed important regulation of dendritogenesis and synaptogenesis during early brain development but also demonstrated a tight link between these early developmental events and cognitive functions later in life.

miR-9 | learning | memory | Diap1 | dendritogenesis

Perturbation during the critical period of perinatal cortical development influences the functional connectivity of the brain and can lead to an increased propensity toward neurological disorders such as anxiety, schizophrenia, and autism spectrum disorders (1–3). Neuronal maturation involves distinct, highly regulated events, including neuronal differentiation and migration, dendritogenesis, axon formation/guidance, and synaptogenesis, among others. However, precisely how these events are regulated and how they orchestrate brain development and cognitive function remain largely unknown.

Fear-related learning and memory play a significant role in the development of anxiety disorders. Cortical dysfunction is associated with emotional disturbances, which are underpinned by impaired fear extinction, and an inefficient termination of physiological stress responses (4, 5). The medial prefrontal cortex (mPFC) is a primary mediator of fear-related learning and memory (6, 7). It is evident that the actin cytoskeleton is involved in synaptic plasticity and neuronal morphogenesis underlying the formation of fear memory. For example, a disruption in the actin cytoskeleton assembly in the adult brain impairs both cued and contextual fear conditioning (8–10), and several actin-regulatory proteins have been shown to be involved in synaptic plasticity and neuronal morphogenesis associated with memory formation (11–15).

Small noncoding RNAs, and miRNAs in particular, have emerged as a major regulatory mechanism that precisely controls the level of gene expression. In invertebrates, miRNAs play essential roles in regulating developmental timing. For example, in *Caenorhabditis elegans* the succession of certain cell fates from first to second larval stage relies on the induction of miRNA lin-4 expression at the first larval stage and reduction of lin-14 activity via base-pairing interactions with its 3′ UTR (16, 17). In mice, miRNAs have been shown to be involved in rapidly fine-tuning the expression of their target mRNAs and in regulating cognitive function (18, 19). In our study, we found that the expression of the actin polymerization regulator diaphanous homologous protein 1 (Diap1) was significantly down-regulated in mouse cortical neurons from E16 to postnatal day 0 (P0), which is concomitant with a critical period of cortical dendritogenesis. We have also shown that the expression of a brain-enriched miRNA, miR-9, was inversely related to the expression of Diap1 (20). Furthermore, we identified a putative miR-9–binding site in the 3′ UTR of Diap1, indicating a potential regulatory relationship between Diap1 and miR-9 during dendritogenesis. These findings prompted an investigation into whether there is a functional relationship between key regulators of the actin cytoskeleton and miR-9 during prenatal development and whether dendritogenesis during the perinatal period will have an impact on cognition in adult life.

Results

Diap1 Regulates Dendritogenesis and Fear-Related Memory. Diap1 belongs to an evolutionarily conserved family of formin-related proteins (21), and binding of profilin (Pfn) to Diap1 mediates fast barbed-end elongation that promotes long, unbranched actin filaments (22). To explore a possible role for Diap1 in neuronal maturation, we analyzed the pattern of cortical Diap1 expression from E12 to adulthood. Diap1 was highly expressed at E12 but progressively decreased to low levels around E18 in cortical neurons. The expression of Diap1 increased again from P1 to P7 and decreased afterward (Fig. 1*A*). In contrast to Diap1, the expression of a brain-specific isoform of Pfn, Pfn2, increased in the prenatal cortex, decreased postnatally, and then remained relatively constant after P7 (Fig. 1*A*). Diap1 expression anti-correlates with the critical period of cortical dendritogenesis after neuronal migration is complete (23).

Significance

This study expands our knowledge of small noncoding RNAs and their important roles in brain development and cognitive function. We describe a mechanism by which dendritic morphology and synaptic formation are altered during a critical period of development, eventually leading to altered capacity for learning and memory later in life.

Author contributions: Q.L. and Y.E.S. designed research; Q.L., R.P., J.W., J.A.C., W.G., C.P., T.B., and T.W.B. performed research; Q.L. contributed new reagents/analytic tools; Q.L., R.P., J.W., J.A.C., C.P., M.L., and T.W.B. analyzed data; and Q.L., T.W.B., M.S.F., K.Y., and Y.E.S. wrote the paper.

The authors declare no conflict of interest.

This article is a PNAS Direct Submission.

[1]To whom correspondence may be addressed. Email: ysun@mednet.ucla.edu or qlin@mednet.ucla.edu.

This article contains supporting information online at www.pnas.org/lookup/suppl/doi:10.1073/pnas.1706069114/-/DCSupplemental.

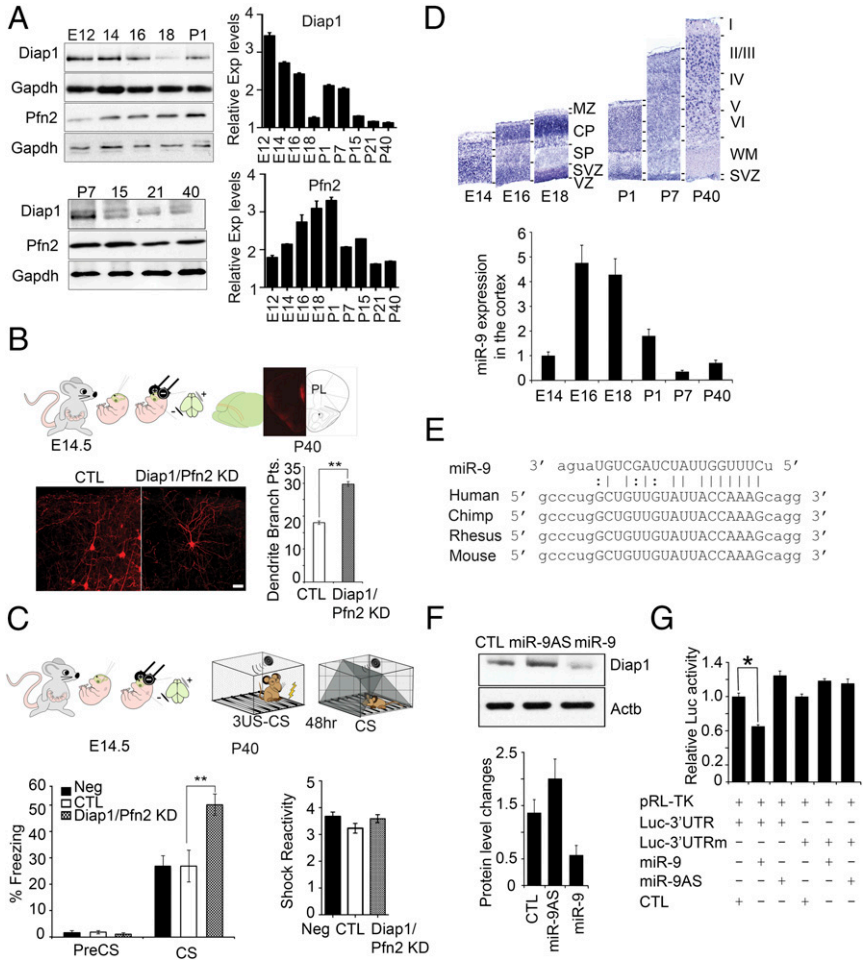

Fig. 1. Diap1 and Pfn2 regulation of dendritic morphology and fear memory is directly regulated by miR-9. (*A*, *Left*) Western blot analysis of the temporal expression of Diap1 and Pfn2 in developing and adult cortices. GAPDH is a loading control. (*Right*) Densitometry analysis of Diap1 and Pfn2 expression. (*B*, *Upper*) Schematic representation of in utero injection of plasmid followed by electroporation into mPFC progenitors at the ventricular zone at E14.5. (Scale bar, 50 μm.) (*Lower*) Knockdown of Diap1/Pfn2 starting from E14.5 increased dendrite complexity in the PL neurons [$^{**}P < 0.01$, Kruskal–Wallis test; control (CTL) $n = 42$ neurons; Diap1/Pfn2 KD $n = 37$ neurons]. (*C*, *Upper*) Schematic representation of in utero injection of plasmid followed by auditory fear conditioning. (*Lower Left*) Knockdown of Diap1/Pfn2 in mPFC facilitated fear memory in adult male mice ($^{**}P < 0.01$, Kruskal–Wallis test; CTL $n = 12$; Diap1/Pfn2 KD $n = 12$). Brains from littermates were fixed and used for anatomic analysis. CTL, control empty plasmid; CS, conditioned stimulus; Diap1/Pfn2 KD, Diap1 and Pfn2 shRNA knockdown constructs; Neg, electroporated without plasmid; US, unconditioned stimulus. (*Lower Right*) Knockdown of Diap1/Pfn2 has no effect on shock sensitivities (Kruskal–Wallis test, $P = 0.6056$; CTL $n = 12$; Diap1/Pfn2 KD $n = 12$). (*D*) ISH (*Upper*) combined with TaqMan-qPCR (*Lower*) analysis of miR-9 expression in mouse cortex from E14–P40. The mature miR-9 was expressed in the ventricular zone (VZ) and subventricular zone (SVZ) from E14 to adult. miR-9 expression reached highest level around E16–E18. miR-9 was expressed in neocortical neurons at a relatively low level postnatally (P7–P40). CP, cortical plate; SP, subplate. (*E*) Conservation of miR-9 target sequences in mammalian Diap1 3′ UTRs. (*F*, *Upper*) Western blot analysis of miR-9 regulation of Diap1 expression. E14.5 cortical neurons were isolated and transfected with miR-9 overexpression, knockdown, or control lentiviral particles [E14.5 + 6 d in vitro (DIV)]. (*Lower*) Densitometry analysis of the Western blotting. (*G*) Relative luciferase activity of reporter genes in miR-9 overexpressed and knocked down HEK293T cells ($^{*}P < 0.05$, Wilcoxon–Mann–Whitney test). Luc-3′UTR, luciferase reporter constructs of miR-9 targets; Luc-3′UTRm, mutant control of miR-9 luciferase reporter construct; pRL-TK, luciferase internal control.

To examine the role of Diap1 and Pfn2 in regulating dendritic morphogenesis in cortical neurons, we delivered Diap1 and Pfn2 shRNAs into neural progenitors in the mouse mPFC at E14.5 by in utero electroporation (Fig. 1*B*, *Upper* and Fig. S1*A*). The in utero electroporation methodology allows specific targeting of neurons in the prelimbic frontal cortex (PL) of the mPFC, an area of the brain that regulates fear-related learning and memory (7). At P40, we imaged PL pyramidal neurons in cortical layers 2/3 and reconstructed them in 3D. The continuous knockdown of Diap1 and Pfn2 from E14.5 to adulthood led to a dramatic increase in dendritic complexity in the PL (Fig. 1*B*, *Lower*).

We examined the effect of Diap1/Pfn2 knockdown on fear memory and found that continuous knockdown of Diap1/Pfn2 in PL neurons significantly enhanced the expression of auditory-cued fear memory (Fig. 1*C*) without changing pain sensitivity (Fig. 1*C*, *Lower Right*). However, we did not observe a dramatic effect on contextual fear memory (Fig. S1*B*). Given that CD-1 mice are low-freezing mice for both tone and context (24, 25), it is possible that we were not able to see an increase in context fear despite the effects of our experimental manipulations on both cue and context fear. Finally, knockdown of Diap1/Pfn2 in the PL did not appear to alter fear acquisition (Fig. S1*C*).

miR-9 Directly Regulates Diap1 Expression. Using in situ hybridization (ISH) combined with immunohistochemistry and qPCR, we found that miR-9 was highly expressed in neural progenitor cells in the germinal zone and within newborn neurons in the cortical plate as early as E14.5 (Fig. 1*D* and Fig. S2*A*) (20). The expression of miR-9 gradually increased, reaching its maximum level at E16–E18. This pattern of expression persisted in cortical neurons and in

subventricular zone progenitors in the postnatal brain (Fig. S2*B*). Intriguingly, this temporal expression pattern exhibited an inverse correlation with the expression pattern of Diap1 before P7 (Fig. 1*A*). Moreover, cortical neurons overexpressing miR-9 formed massive lamellipodia-like structures around the soma (Fig. S2*C*, *Upper*). Overexpression of miR-9 in mouse embryonic fibroblasts (MEFs) led to a disorganized pattern of F-actin filaments (Fig. S2*C*, *Lower*), which somewhat mimicked the phenotype of F-actin cytoskeleton in HeLa cells expressing deficient Diap1 (26). We further identified an evolutionarily conserved miR-9–binding site in the 3′ UTR of Diap1 mRNA in different species (www.targetscan.org/vert_71/ and www.microrna.org/microrna/home.do) (Fig. 1*E*).

To examine whether there is a functional interaction between miR-9 and Diap1, we analyzed protein levels of Diap1 in cultured neocortical neurons by overexpressing or knocking down miR-9. We found that overexpression of miR-9 decreased Diap1 protein levels by 60%. Conversely, knockdown of miR-9 (miR-9AS) in cultured cortical neurons increased Diap1 protein levels by 50–80% (Fig. 1*F*). Using a luciferase reporter assay, we found Diap1 to be a direct target of miR-9 (Fig. 1*G* and Fig. S3*A*). Moreover, overexpression or knockdown of miR-9 in cultured cortical neurons did not significantly alter the expression levels of related actin cytoskeleton regulators such as WAS protein family member 2 (Wave2), Rho/Rac guanine nucleotide exchange factor 2 (Arhgef2), actin-related protein 2/3 complex, subunit 1A (Arpc1a), protein phosphatase 1, regulatory subunit 12A (pPP1R12A), and P21 protein (Cdc42/Rac)-activated kinase 4 (PAK4), which have predicted miR-9–binding sites in their mRNA 3′ UTRs (Fig. S3*B*). Interestingly, although Pfn2 expression does not anti-correlate with miR-9 expression in either developing or adult cortices, miR-9 overexpression in cultured E14.5 cortical neurons still significantly down-regulates Pfn2 expression, suggesting that, although miR-9 can regulate Pfn2 expression, Pfn2 is also under the regulation of additional factors irrelevant to miR-9 (Fig. S3 *C* and *D*).

miR-9 Regulates Dendritic Structure and Synaptic Formation During Early Brain Development and Influences Fear Memory in Adult Mice. To elucidate the role of miR-9 in the regulation of fear-related learning and memory, we delivered miR-9 overexpression, knockdown, or the control plasmid, respectively, into PL progenitors at E14.5 by in utero electroporation. At P40, an auditory-cued fear-conditioning test revealed a significant enhancement of the expression of fear memory in mice that had been electroporated with the miR-9 overexpression construct. Conversely, knockdown of miR-9 prevented the formation of fear memory in adult mice (Fig. 2*A*, *Left*). There was no effect on contextual fear memory (Fig. S4*A*). Fear acquisition and foot-shock reactivity did not differ among miR-9, miR-9AS, and control groups (Fig. 2*A*, *Right* and Fig. S4*B*). These data demonstrate that miR-9, a negative regulator for Diap1, also regulates fear memory.

We subsequently examined whether exogenous miR-9 overexpression from E14.5 would lead to any changes in dendritic morphology as well as synaptogenesis of PL neurons. At P40 we imaged PL pyramidal neurons in cortical layers 2/3 and reconstructed them in 3D. In agreement with the Diap1 and Pfn2 double-knockdown data, overexpression of miR-9 from E14.5 led to an increase in the number of dendrite branch points in PL neurons and in cultured cortical neurons, whereas knockdown of endogenous miR-9 or overexpression of Diap1 (lack of the miR-9–binding sequence) led to a significant reduction in the number of dendrite branch points (Fig. 2*B* and Fig. S5). Importantly, we found that overexpression of miR-9 increased synaptic density in PL neurons. In contrast, knockdown of miR-9 or overexpression of Diap1 impaired synaptic formation (Fig. 2*C*). Moreover, we showed that miR-9 increased the number of dendritic spines, whereas knockdown of miR-9 or overexpression Diap1 decreased their number (Fig. 2*D*). Taken together, these data demonstrate an essential role for miR-9 and Diap1 in the regulation of dendritic morphogenesis and synaptogenesis in the developing brain that may contribute to fear learning and memory later in life.

Coexpression of Diap1 Rescues the Dendritic Phenotype as Well as Alterations in Fear-Related Learning and Memory Deficit Elicited by miR-9 Overexpression. To determine whether miR-9 indeed functions as a negative regulator for Diap1, we carried out rescue experiments to examine the effects of coexpression of Diap1 and miR-9 on dendritic morphogenesis and synaptic formation in cortical neurons. The mRNA of the overexpressed Diap1 lacks the miR-9 3′ UTR binding site (Fig. S6). We showed that coexpression of Diap1 and miR-9 normalized dendritic branching morphology in both primary cortical neurons and in the pyramidal neurons of PL layers 2/3. Overexpression of miR-9 increased dendritic complexity, whereas overexpression of Diap1 alone in cortical neurons reduced dendritic branch points in vitro and in vivo (Fig. 3 *A* and *B*). Quantification of synapses revealed a reversal of the number of synaptic puncta to control levels in cultured cortical neurons that coexpressed exogenous Diap1 and miR-9. Knockdown of miR-9 and overexpression of Diap1 reduced the number of synapses (Fig. 3*C*). We further demonstrated that co-overexpression of Diap1 with miR-9 in the PL reverses the freezing phenotype that resulted from either miR-9 or Diap1 overexpression alone (Fig. 3*D*).

Interestingly, knockdown of Pfn2 alone does not significantly enhance animal freezing behavior, whereas knocking down Diap1 alone and only during the developmental period (E14.5–P0) via a doxycycline (Dox)-inducible driver is sufficient to promote dendritic complexity and facilitate fear-memory–related freezing behavior (Figs. S7 and S8). Moreover, restricted overexpression of miR-9 only during development (E14.5–P0) is also sufficient to lead to increased dendritic complexity in the PL neurons and enhanced fear memory (Figs. S7 and S8). Taken together, although both Pfn2 and Diap1 are bona fide targets for miR-9, only Diap1 mainly functions in regulating fear memory. In addition, our data clearly demonstrate a tight functional link between Diap1 and its modulator miR-9 in establishing neural circuits during the critical period of neuronal development. Perturbation of this process has life-long effects on fear-related learning and memory.

Discussion

Neurodevelopmental disorders can be triggered by environmental and genetic interference with normal brain development. It is well established that there are critical time windows for the establishment of certain types of neural plasticity, and at those times individuals are most vulnerable to external disturbances (27–30). In the current study we provided evidence that miR-9 and Diap1 function as part of an intrinsic program that guides the process of neuronal maturation (i.e., dendritogenesis and synaptogenesis) and has long-lasting effects on dendritic complexity and synaptic density in adulthood. Furthermore, to provide some temporal specificity, we used a Dox-inducible system to knock down only Diap1 or miR-9 or to overexpress miR-9 during the early developmental period, i.e., from E14.5 to P0, and found that temporally restricted perturbation of the miR-9–Diap1 axis was sufficient to provide long-lasting effects in dendritic morphology and fear-related learning and memory behavior (Figs. S7 and S8). These data suggest that a disruption in an intrinsic developmental program from the midembryonic stage has a significant impact on cognitive function in adult life.

Our previous and the current studies have shown that overexpressed miR-9 binds exclusively to endogenous target sequences, although it does not target to its binding sequence with seed-sequence mutations (Fig. 1*G*). To test the specificity of the miR-9 overexpression construct further, we built miR-9 scramble control (miR-9SC). The scramble sequence of the miR-9 mature sequence was generated using online software (www.genscript.com/tools/create-scrambled-sequence). Using overlapping PCR, the mature miR-9 and its 3p sequences of the original genomic sequence were replaced by its scrambled and scrambled-complementary sequences, respectively (Fig. S9*A*) (31). The sequence was introduced into the same backbone vector as the miR-9 overexpression vector. In the luciferase assay we found that, as with the empty vector, the scrambled sequence did not bind to miR-9–binding sequence (Fig. S9*B*).

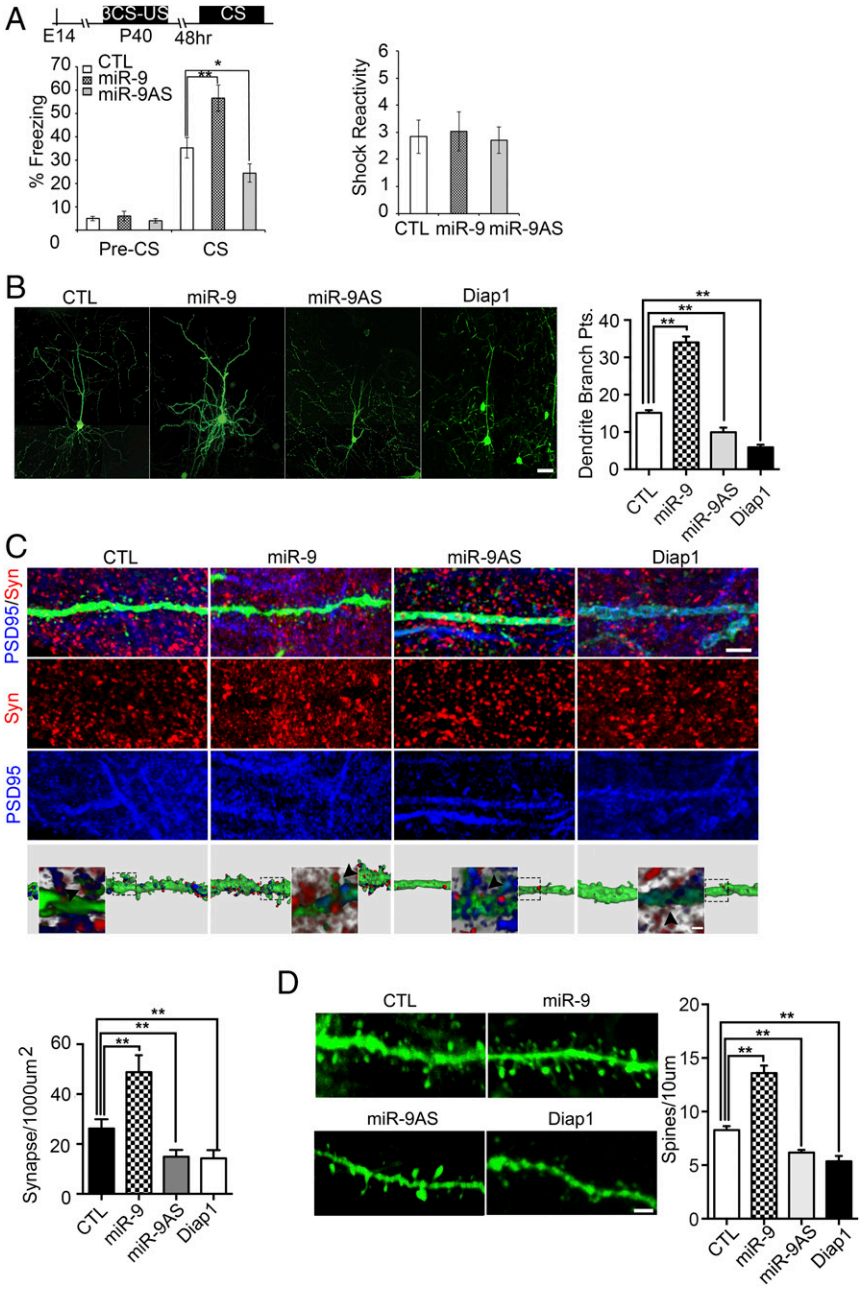

Fig. 2. miR-9 modulates dendritic morphogenesis, number of synaptic puncta, and spin density that may contribute to memory formation. (*A*, *Left*) Cued fear memory is significantly enhanced in mice that had been electroporated with miR-9 at E14.5. miR-9AS administered at E14.5 prevented the formation of fear memory in adult mice (**$P < 0.01$, *$P < 0.05$, Kruskal–Wallis test; CTL $n = 16$; miR-9 $n = 8$, miR-9AS $n = 12$). (*Right*) Shock sensitivity did not differ among different groups (Kruskal–Wallis test, $P = 0.8208$; CTL $n = 16$; miR-9 $n = 8$; miR-9AS $n = 12$). (*B*) Overexpression or knockdown of miR-9 or overexpression of Diap1 in PL cortical neurons starting from dendritogenesis altered dendritic morphology (*$P < 0.05$, **$P < 0.01$, Kruskal–Wallis test; CTL $n = 29$ neurons; miR-9 $n = 33$ neurons; miR-9AS $n = 30$ neurons; Diap1 $n = 44$ neurons).(Scale bar, 40 μm.) Diap1, Diap1 overexpression construct. (*C*, *Upper*) Overexpression or knockdown of miR-9 or overexpression of Diap1 starting from E14.5 in PL cortical neurons altered synaptic formation (**$P < 0.01$, Kruskal–Wallis test; CTL $n = 14$ neurons; miR-9 $n = 17$ neurons; miR-9AS $n = 16$ neurons; Diap1 $n = 14$ neurons). Shown are examples of a dendrite (GFP^+) stained with synaptic markers. (Scale bar, 5 μm.) Presynaptic terminals were identified by staining for synapsin (Syn, red). Postsynaptic structures were identified by staining for postsynaptic density protein 95 (PSD95, blue). Synapses were identified by the close proximity of pre- and postsynaptic elements (≤0.5 μm, arrowheads in the bottom images). (*Lower*) 3D construction of PSD-95 (blue) and presynaptic synapsin (red) identified using the "create spots" algorithm in Imaris. *Insets* show boxed areas at high magnification. (Scale bar, 1 μm.) (*D*, *Left*) Quantification of the number of protrusions per 10 μm of dendrites. (Scale bar, 2 μm.) (*Right*) Overexpression or knockdown of miR-9 or overexpression of Diap1 in PL cortical neurons affected dendritic spine formation (**$P < 0.01$, Mann–Whitney test; CTL, $n = 28$ neurons; miR-9 $n = 42$ neurons; miR-9AS $n = 38$ neurons; Diap1 $n = 19$ neurons).

Moreover, overexpression of the miR-9SC does not alter dendritic morphology or synapse formation (Fig. S9 *C* and *D*). To determine miR-9 knockdown specificity, we constructed a mutant form of the miR-9 knockdown control by replacing the seed-binding sequence with a random sequence (Fig. S9*A*). A luciferase assay showed that overexpression of the miR-9 knockdown mutant fragment (miR-9ASMut) did not interfere with luciferase gene expression (Fig. S9*B*). We further showed that overexpression of miR-9ASMut did not affect dendritic branching or synaptic formation (Fig. S9 *C* and *D*), suggesting that the miR-9 knockdown sponge configuration is specific.

We do have concern that the overexpression of small RNAs may, by itself, have certain cellular and organismic effects that may not depend solely on the specific sequences used. For example, it is possible that overexpression of any exogenous DNA fragment (i.e., GFP, ion channels, noncoding RNAs) in a hemostatic biological system may have some unwanted effects, such as attenuating the transcription and translation machineries of other endogenous genes, changing a cell's physiological properties. However, with the extensive series of controls described above, we concluded that the nonspecific effects of miR-9 overexpression or knockdown configurations, if any, could contribute little, if at all, to the biological effect we observed. In addition, we are fully aware of the potential off-target issue associated with the shRNA knockdown approach (32). Our Diap1 overexpression and knockdown assays showed that Diap1 regulates dendritogenesis, synapse formation, and fear-related learning and memory. With both constant and temporally restricted gain- and loss-of-function approaches targeting two related endogenous components (Diap1 and miR-9) pointing to the same conclusion, we are confident that miR-9 plays an essential role in the regulation of Diap1 gene expression. Misregulation of miR-9 and Diap1 interaction during the critical period of dendritogenesis led to abnormalities in dendritic complexity and the establishment of neural circuitry, with substantial effects on fear learning and memory later in life. More importantly, Diap1–miR-9 rescue assays showed the

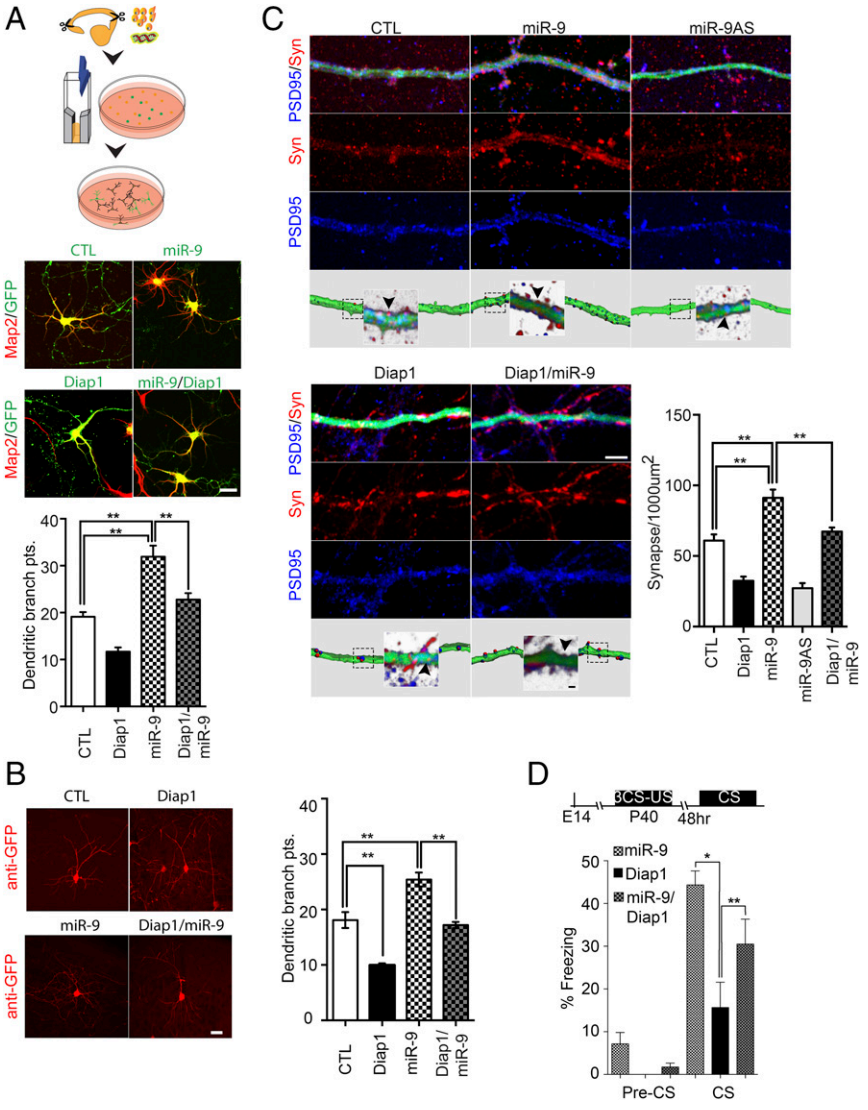

Fig. 3. Coexpression of Diap1 in miR-9–overexpressing cortical neurons normalizes the number of dendritic branches and synaptic puncta and the increased fear memory elicited by the overexpression of miR-9. (*A* and *B*) Coexpression of Diap1 and miR-9 in cortical neurons rescued the dendritic morphology in cultured cortical neurons (CTL $n = 13$; Diap1 $n = 23$; miR-9 $n = 16$; miR-9/Diap1 $n = 22$) (*A*) and in the PL pyramidal neurons in mice (CTL $n = 10$; Diap1 $n = 66$; miR-9 $n = 19$; miR-9/Diap1 $n = 34$) (*B*). $^{**}P < 0.01$, Kruskal–Wallis test. Anti-GFP immunostaining is shown in red. (Scale bars, 40 μm.) (*C*) Quantification of synapse in cultured cortical neurons visualized by immunocytochemistry. Overexpression or knockdown of miR-9 or overexpression of Diap1 starting from E15 altered synaptic formation in cortical neurons. Coexpression of miR-9 in Diap1-overexpressing cortical neurons elevated the number of synaptic puncta in cortical neurons. (Scale bar, 5 μm.) *Insets* in the bottom panels show the boxed area at high magnification. (Scale bar, 1 μm.) $^{**}P < 0.01$, Kruskal–Wallis test. (*D*) Coexpression of Diap1 and miR-9 in mPFC cortical neurons reduced the increase in freezing level elicited by the overexpression of miR-9 alone in an auditory fear-conditioning paradigm (Kruskal–Wallis test, $^{*}P < 0.05$, $^{**}P < 0.01$; miR-9 $n = 6$; Diap1 $n = 4$; Diap1/miR-9 $n = 12$).

function of Diap1 in regulating dendritogenesis, synaptic formation, and fear-related learning and memory (Fig. 3). It remains to be determined whether indirect effects of the overexpression or knockdown of miR-9 or Diap1 on their neighborhood neurons contribute to the neuronal morphology and behavioral phenotypes. In agreement with emerging findings on the important role of noncoding RNAs in rapidly shaping phenotypic outcomes in response to current environmental demands, our findings suggest that perturbation of miR-9 activity during early-life events can elicit sensitization toward subsequent stressors later in life and that this sensitization is manifested as enhanced fear-related learning in adulthood.

Materials and Methods

Plasmid Constructions. The constructs of the miR-9 overexpression lentiviral plasmid and the miR-9 antisense sponge were built as described in our previous study (20) using Diap1 and pfn2 3′ UTR fragments with predicted miR-9–binding sites that were inserted immediately downstream of the luciferase reporter vector, pIS0. To regulate the timing of miR-9, Diap1, and Pfn2 expression, a miR-9–2 premiRNA fragment, miR-9 bulged antisense oligo-duplex, Diap1 shRNA, or Pfn2 shRNA was inserted downstream of a pTight/U6 promoter of tetON plasmids pSingle-tTs-shRNA and pLenti7.3. To build a miR-9 reporter construct, a short-lived eGFP, d2eGFP, was inserted into a pCAG-RFP-CMV vector to create the pCAG-RFP-CMV-d2eGFP construct. Three miR-9–binding sites then were inserted immediately downstream of d2eGFP to create the pCAG-RFP-CMV-d2eGFP-miR-9 AM reporter vector. To overexpress Diap1, Diap1 was PCR amplified from the MGC cDNA clone (Thermo Scientific) and subcloned to a modified plasmid, FUIGW. To test the specificity of the miR-9 overexpression and miR-9 knockdown constructs, we built miR-9SC and miR-9ASMut (Fig. S9). See *SI Materials and Methods* for additional details.

Subjects. For in utero electroporation experiments, E14 ICR CD-1 mice were used (Charles River Laboratories). All behavior testing was conducted when the mice were 5–6 wk old, during the light phase in illuminated testing rooms following protocols approved by the Institutional Animal Care and Use Committee of the University of California, Los Angeles.

ISH. ISH assays were carried out as described by Zhao et al. (20). See *SI Materials and Methods* for additional details.

Western Blot Analysis. The whole cerebral cortex was lysed in 0.7% Nonidet P-40 lysis buffer with 1 mM phenylmethylsulfonyl fluoride (PFSF), 10 mM DTT, and a mixture of protease inhibitors. The antibodies used for Western blotting were rabbit anti-Diap1 (1:1,000; Abcam); mouse anti-Pfn2 antibody (1:500; Santa Cruz); mouse anti–β-actin (1:2,000; Sigma); rabbit anti-WAVE2 (1:1,000; Cell Signaling); rabbit anti–GEF-H1 (Arhgef2) (1:1,000), rabbit anti-PAK4 antibody (1:1,000), and mouse anti-MYPT1 (Ppp1r12a) (1:1,000; BD Bioscience); goat anti-Arpc1a (1:1,000; Abnova); mouse anti–β-actin (1:2,000; Sigma); and mouse anti-GAPDH (1:4,000; GeneTex).

Immunohistochemistry. The primary antibodies used in this study were rabbit anti–T-box brain 1 antibody (Tbr1) (1:2,000; EMD Millipore); rabbit anti–T-box

brain 2 antibody (Tbr2) (1:2,000; Millipore); mouse anti-Pax6 antibody (1:500; The Developmental Studies Hybridoma Bank); rabbit anti-GFP antibody (1:2,000; MBL); rabbit anti-PSD95 and mouse anti-synapsin antibodies (1:1,000; Synaptic Systems); guinea pig anti-PSD95 (1:1,000; Synaptic Systems); and guinea pig anti-synapsin (1:1,000; Synaptic Systems). Images were processed with software Imaris (Bitplane).

miRNA TaqMan-qPCR. Total RNAs were extracted from the whole cerebral cortex of E14–P40 CD-1 mice or from in vitro-cultured cortical neurons. RT-PCR and qPCR were described in our previous study (20).

Luciferase Assay. Details are given in *SI Materials and Methods*.

Primary Neuronal Transformation. Details are given in *SI Materials and Methods*.

Administration of Dox. Dox was administrated in the animal's drinking water at a concentration of 2 mg/mL (33).

In Utero Electroporation. The in utero electroporation procedure was carried out as described by Zhao et al. (20). We electroporated the plasmid to a single side of the prelimbic cortex.

Dendrite, Dendritic Spine, and Synaptic Puncta Imaging and Image Processes. The entire profile of each GFP-labeled neuron to be quantified was acquired using a 25× oil immersion objective without optical zoom, NA = 0.8 (Plan-Apochromat; Zeiss). The dendritic branch point is defined as the number of branch bifurcations in the shortest path from the beginning point to a given point in the dendritic graph. Dendrites of individual neurons for each condition were drawn manually and calculated using the Filament function of Imaris software. The dendritic spines were acquired using a 63× oil immersion objective lens, NA = 1.4 (Planapo; Zeiss). The spines were analyzed as described by Swanger and Bassell (34). The synaptic puncta were acquired using a 63× oil immersion objective lens, NA = 1.4 (Planapo; Zeiss) at a resolution of 1,024 × 512 pixels. A z-step of 0.2-μm intervals was used. The pre- and postsynaptic puncta were analyzed as described by Fogarty et al. (35). See *SI Materials and Methods* for additional details.

Fear Conditioning. Cued fear was induced with three pairings of a 2-min, 80-dB, white-noise conditional stimulus (CS) coterminating with a 2-s, 0.4-mA foot shock followed by a 2-min intertrial interval (ITI). Two days after fear acquisition all mice were tested in context B. After a 2-min acclimation, freezing was assessed during two 2-min CS presentations See *SI Materials and Methods* for additional details.

Pain Sensitivity Assays. We assessed the pain processing by analyzing shock reactivity during the shock in fear conditioning. The unconditioned response to shock was examined by a motion index of each animal during footshock (Video Freeze Software; Med Associates).

Histology. At the completion of behavioral testing (for all experiments), the brains were fixed and sectioned. The mice with a majority GFP- or RFP-labeled cells in the PL of the mPFC were used for behavior analysis.

Statistical Analysis. All statistical significance was assessed using an alpha level of 0.05. Statistical analysis was performed using SAS 9.2 and/or GraphPad Prism software.

ACKNOWLEDGMENTS. We thank the Intellectual and Developmental Disabilities Research Center (IDDRC) at the University of California, Los Angeles (UCLA) supported by NIH Grant U54HD087101-02, Donna Crandall of the UCLA-IDDRC Media Core for help with the figures, and Rowan Tweedale for helpful editing. This work was supported by Basic Research Program of China Grants 2012CB966303, 2014CB964602, and 31471009 (to Y.E.S. and Q.L.). Q.L. is the recipient of the 2009 Richard Heyler Award and a 2012 Brain & Behavior Research Foundation NARSAD Young Investigator Grant. J.W. is the recipient of Australian Research Council Discovery Early Career Researcher Award (DECRA) DE170100112. Funding was also provided by NIH/National Institute of Mental Health (NIMH) Grant R01MH084095 and by Chinese National Natural Science Foundation Grants 31271371, 91319309, 2016YFA0100801, and 31620103904 (to Y.E.S.); by NIMH Grant R01MH62122 (to M.S.F.); and by Australian National Health and Medical Research Council Grant GNT1069570 (to T.W.B.).

1. Li J, et al. (2009) A nationwide study on the risk of autism after prenatal stress exposure to maternal bereavement. *Pediatrics* 123:1102–1107.
2. Rapoport JL, Addington AM, Frangou S, Psych MR (2005) The neurodevelopmental model of schizophrenia: Update 2005. *Mol Psychiatry* 10:434–449.
3. Vallée M, et al. (1997) Prenatal stress induces high anxiety and postnatal handling induces low anxiety in adult offspring: Correlation with stress-induced corticosterone secretion. *J Neurosci* 17:2626–2636.
4. Feder A, Nestler EJ, Charney DS (2009) Psychobiology and molecular genetics of resilience. *Nat Rev Neurosci* 10:446–457.
5. Fanselow MS, Poulos AM (2005) The neuroscience of mammalian associative learning. *Annu Rev Psychol* 56:207–234.
6. Quinn JJ, Ma QD, Tinsley MR, Koch C, Fanselow MS (2008) Inverse temporal contributions of the dorsal hippocampus and medial prefrontal cortex to the expression of long-term fear memories. *Learn Mem* 15:368–372.
7. Sierra-Mercado D, Padilla-Coreano N, Quirk GJ (2011) Dissociable roles of prelimbic and infralimbic cortices, ventral hippocampus, and basolateral amygdala in the expression and extinction of conditioned fear. *Neuropsychopharmacology* 36:529–538.
8. Fischer A, Sananbenesi F, Schrick C, Spiess J, Radulovic J (2004) Distinct roles of hippocampal de novo protein synthesis and actin rearrangement in extinction of contextual fear. *J Neurosci* 24:1962–1966.
9. Rehberg K, Bergado-Acosta JR, Koch JC, Stork O (2010) Disruption of fear memory consolidation and reconsolidation by actin filament arrest in the basolateral amygdala. *Neurobiol Learn Mem* 94:117–126.
10. Motanis H, Maroun M (2012) Differential involvement of protein synthesis and actin rearrangement in the reacquisition of contextual fear conditioning. *Hippocampus* 22:494–500.
11. Lamprecht R, Farb CR, LeDoux JE (2002) Fear memory formation involves p190 RhoGAP and ROCK proteins through a GRB2-mediated complex. *Neuron* 36:727–738.
12. Diana G, et al. (2007) Enhancement of learning and memory after activation of cerebral Rho GTPases. *Proc Natl Acad Sci USA* 104:636–641.
13. Saitoh A, et al. (2006) ROCK inhibition produces anxiety-related behaviors in mice. *Psychopharmacology (Berl)* 188:1–11.
14. Meng Y, et al. (2002) Abnormal spine morphology and enhanced LTP in LIMK-1 knockout mice. *Neuron* 35:121–133.
15. Rust MB, et al. (2010) Learning, AMPA receptor mobility and synaptic plasticity depend on n-cofilin-mediated actin dynamics. *EMBO J* 29:1889–1902.
16. Lee RC, Feinbaum RL, Ambros V (1993) The *C. elegans* heterochronic gene lin-4 encodes small RNAs with antisense complementarity to lin-14. *Cell* 75:843–854.
17. Wightman B, Ha I, Ruvkun G (1993) Posttranscriptional regulation of the heterochronic gene lin-14 by lin-4 mediates temporal pattern formation in *C. elegans*. *Cell* 75:855–862.
18. Lin Q, et al. (2011) The brain-specific microRNA miR-128b regulates the formation of fear-extinction memory. *Nat Neurosci* 14:1115–1117.
19. Nudelman AS, et al. (2010) Neuronal activity rapidly induces transcription of the CREB-regulated microRNA-132, in vivo. *Hippocampus* 20:492–498.
20. Zhao J, et al. (2015) Ngn1 inhibits astrogliogenesis through induction of miR-9 during neuronal fate specification. *Elife* 4:e06885.
21. Watanabe N, et al. (1997) p140mDia, a mammalian homolog of *Drosophila* diaphanous, is a target protein for Rho small GTPase and is a ligand for profilin. *EMBO J* 16:3044–3056.
22. Watanabe N, Higashida C (2004) Formins: Processive cappers of growing actin filaments. *Exp Cell Res* 301:16–22.
23. Barnes AP, Polleux F (2009) Establishment of axon-dendrite polarity in developing neurons. *Annu Rev Neurosci* 32:347–381.
24. Valentinuzzi VS, et al. (1998) Automated measurement of mouse freezing behavior and its use for quantitative trait locus analysis of contextual fear conditioning in (BALB/cJ x C57BL/6J)F2 mice. *Learn Mem* 5:391–403.
25. Sartori SB, et al. (2011) Enhanced fear expression in a psychopathological mouse model of trait anxiety: Pharmacological interventions. *PLoS One* 6:e16849.
26. Watanabe N, Kato T, Fujita A, Ishizaki T, Narumiya S (1999) Cooperation between mDia1 and ROCK in Rho-induced actin reorganization. *Nat Cell Biol* 1:136–143.
27. Lupien SJ, McEwen BS, Gunnar MR, Heim C (2009) Effects of stress throughout the lifespan on the brain, behaviour and cognition. *Nat Rev Neurosci* 10:434–445.
28. Hartley CA, Lee FS (2015) Sensitive periods in affective development: Nonlinear maturation of fear learning. *Neuropsychopharmacology* 40:50–60.
29. Cicchetti D (2015) Neural plasticity, sensitive periods, and psychopathology. *Dev Psychopathol* 27:319–320.
30. Hubel DH, Wiesel TN (1970) The period of susceptibility to the physiological effects of unilateral eye closure in kittens. *J Physiol* 206:419–436.
31. Bryksin AV, Matsumura I (2010) Overlap extension PCR cloning: A simple and reliable way to create recombinant plasmids. *Biotechniques* 48:463–465.
32. Grimm D, et al. (2006) Fatality in mice due to oversaturation of cellular microRNA/short hairpin RNA pathways. *Nature* 441:537–541.
33. Cawthorne C, Swindell R, Stratford IJ, Dive C, Welman A (2007) Comparison of doxycycline delivery methods for Tet-inducible gene expression in a subcutaneous xenograft model. *J Biomol Tech* 18:120–123.
34. Swanger SA, Bassell GJ (2011) Making and breaking synapses through local mRNA regulation. *Curr Opin Genet Dev* 21:414–421.
35. Fogarty MJ, Hammond LA, Kanjhan R, Bellingham MC, Noakes PG (2013) A method for the three-dimensional reconstruction of Neurobiotin™-filled neurons and the location of their synaptic inputs. *Front Neural Circuits* 7:153.